IPFR

Institute of Plasma
and Fusion Research

Computer Simulation of the Dissotron Instability

S.T. Ness and G.L. Morales

October 1994 PPG 1522

Affiliated with the Departments of:

Astronomy
Earth and Space Sciences
Electrical Engineering
Materials Science and Engineering
Mechanical, Aerospace and Nuclear Engineering
Physics

and

Center for Advanced Accelerators
Institute of Geophysics and Planetary Physics

UNIVERSITY OF CALIFORNIA • LOS ANGELES

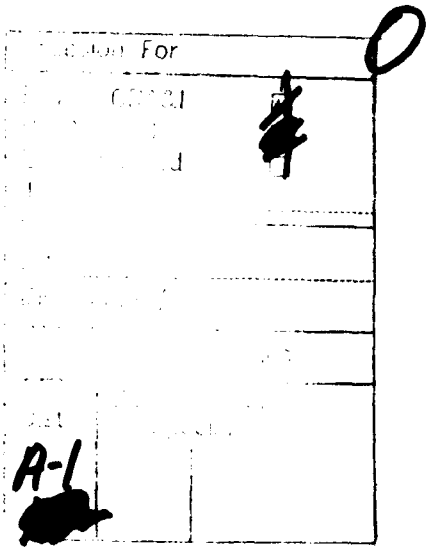

Computer Simulation of the Diocotron Instability

S.C. Neu and G.J. Morales

October 1994 PPG-1522

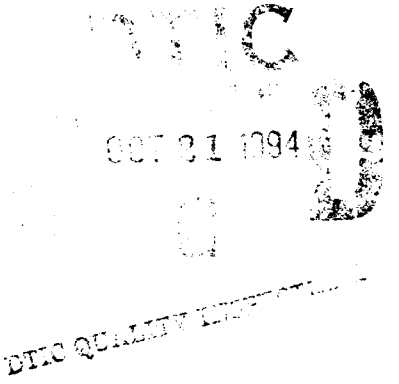

University of California at Los Angeles
Department of Physics
Los Angeles, CA 90024-1547

To Appear in the Proceedings of the Nonneutral Plasma Workshop, 1994

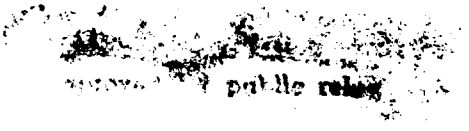

COMPUTER SIMULATION OF THE DIOCOTRON INSTABILITY

S. C. Neu and G. J. Morales
Physics Department, University of California, Los Angeles,
Los Angeles, CA 90024

OVERVIEW

A particle simulation study demonstrates that an initial-value analysis is essential in understanding the early-time growth of diocotron modes. It is also demonstrated that the equilibrium properties of a rigid rotor (including rotation on both the high and the low frequency branches) are well described by particle simulation.

NONNEUTRAL PARTICLE SIMULATION CODE

An electrostatic, particle-in-cell code[1,2] is used to model the behavior of a strongly magnetized, nonneutral system in the plane (x,y) perpendicular to the confining magnetic field (along z). The system is bounded by two planar walls (located at $x = \pm a$) on which the value of the potential is zero (ground). The code is 2-1/2 dimensional, i.e., it follows 3 velocity components (v_x,v_y,v_z) and two spatial coordinates (x,y) on a time scale smaller than a gyroperiod. Time is scaled to the spatially averaged $< \omega_{pe}^2 >^{-1/2}$. The y coordinate is periodic (with length L) and the z-variation is ignorable. In this study we consider two different initial configurations: a nonneutral plasma slab parallel to the walls, and a small rotating cylinder far from the walls.

EVOLUTION OF A NONNEUTRAL PLASMA SLAB

A pure electron plasma slab having uniform density and width $2r_p$ is centered between the walls at $t = 0$. The slab is initialized by giving each electron an initial velocity $v_y(t{=}0) = \omega_{pe}^2 x/\Omega_e$, corresponding to the expected $\underline{E} \times \underline{B}$ drift. A small random velocity is added to yield a low temperature Maxwellian in the drift frame. The system is divided into 32 grids along x and 1024 grids along y. More than 32,000 particles are typically followed, and the system is well below the Brillouin limit; i.e., $\Omega_e/\omega_{pe} = 6$.

Figure 1a shows the configuration space during the early stage of the diocotron instability and Figure 1b exhibits the formation of vortices at a later time. The time evolution of each Fourier mode (having $k_n = 2\pi n/L$) is monitored using the potential along $x = 0$. It is found that there is an inherent mixture of transient and beat behavior which can be confused with an instability or a nonlinear mode-coupling process. This phenomenon is illustrated in Fig. 2, where the solid curves correspond to the simulation results. Figure 2a shows that mode

20 exhibits a monotonic exponential growth, while Fig. 2b shows that mode 26 also grows initi[illegible]ut is followed by an abrupt drop ($t > 15$) in amplitude. The initial grow[illegible] Fig. 2b arises both because of transients and because of the beat between two surface modes (one on the top interface and the other on the bottom) moving past each other. A proper description of the phenomenon requires an initial-value analysis too lengthy to report here. The method uses a Laplace transform to generate a differential equation in x which is solved via a Green's function using the method of Case[3]. The inverse transform is obtained by evaluating the residues, but one remaining integration over x must be done numerically. The result of this analysis is indicated by the dashed lines in Fig. 2. It is evident that mode 20 corresponds to a true instability, while the unusual evolution of mode 26 is a transient feature not contained in the steady-state stability analysis.

The growth rates of the unstabl[illegible] observed in the simulation are shown in Fig. 3. These growth rates are m[illegible]ed by recording the potential energy of each simulation mode over a finite time interval. The solid curve is the well-known[4] expression for the growth rate γ of an unstable mode (of wave number k) of a slab of width $2r_p$ in the limit $a \to \infty$:

$$\frac{\gamma}{\omega_{pe}} = \frac{\omega_{pe}}{2\Omega_e}\sqrt{e^{-4kr_p} - (1 - 2kr_p)^2}. \tag{1}$$

Excellent agreement between the asymptotic theory and the simulation results is obtained over a wide range. The possible discrepancies associated with the high-k modes (18-21) are likely to be due to the sampling of the growth rates at early times. The initial-value theory shows that early in time these growth rates are larger than their asymptotic values. We have also simulated systems with different ratios of r_p/a and found excellent agreement with the theoretical predictions. As $r_p/a \to 1$, the system remains stable, as expected.

RIGID ROTOR EQUILIBRIUM

We have investigated the behavior of a small rigid rotor of radius r_0 bounded by planar walls ($r_0/a \simeq 0.16$) as sketched in Fig. 4. The magnetic field strength B_0 has been varied over the range $1.5 \leq \Omega_e/\omega_{pe} \leq 3$ in order to measure the equilibrium rotation frequencies and the radial oscillation frequencies. For each choice of B_0 the system is initialized by assigning to each particle an azimuthal velocity $r\omega_{re}$, to which a small random component is added to represent a small thermal spread, and where

$$\frac{\omega_{re}}{\Omega_e} = \frac{1}{2} \pm \frac{1}{2}\sqrt{1 - \frac{2\omega_{pe}^2}{\Omega_e^2}}, \tag{2}$$

corresponds to the two possible rotation frequencies for a rigid rotor in vacuum. The average radius and average rotation frequency of the cylinder are monitored

as a function of time. It is found that the rotor exhibits long-term stable oscillations in both the mean radius and the mean rotation frequency. The top of Fig. 4 shows that the simulated system follows the classical rotation diagram, while the bottom shows that the frequencies of the radial oscillations follow the solid curve predicted by the magnetron frequency

$$\frac{\omega_{mag}}{\Omega_e} = \sqrt{1 - \frac{\omega_{pe}^2}{\Omega_e^2}}. \tag{3}$$

ACKNOWLEDGMENTS

This work is sponsored by the Office of Naval Research. Drs. V. K. Decyk and H. Ramachandran played a key role in the development of the computer code.

REFERENCES

1. H. Ramachandran, G. J. Morales, and V. K. Decyk, Phys. Fluids B **5**, 2733 (1993).

2. C. K. Birdsall and A. B. Langdon, *Plasma Physics via Computer Simulation* (McGraw-Hill, New York, 1985).

3. K. M. Case, Phys. Fluids **3**, 143 (1960).

4. For example, O. Buneman, R. H. Levy, and L. M. Linson, J. Appl. Phys. **37**, 3203 (1966).

5. R. C. Davidson, *Physics of Nonneutral Plasmas* (Addison-Wesley, Redwood City, CA, 1990), p. 41.

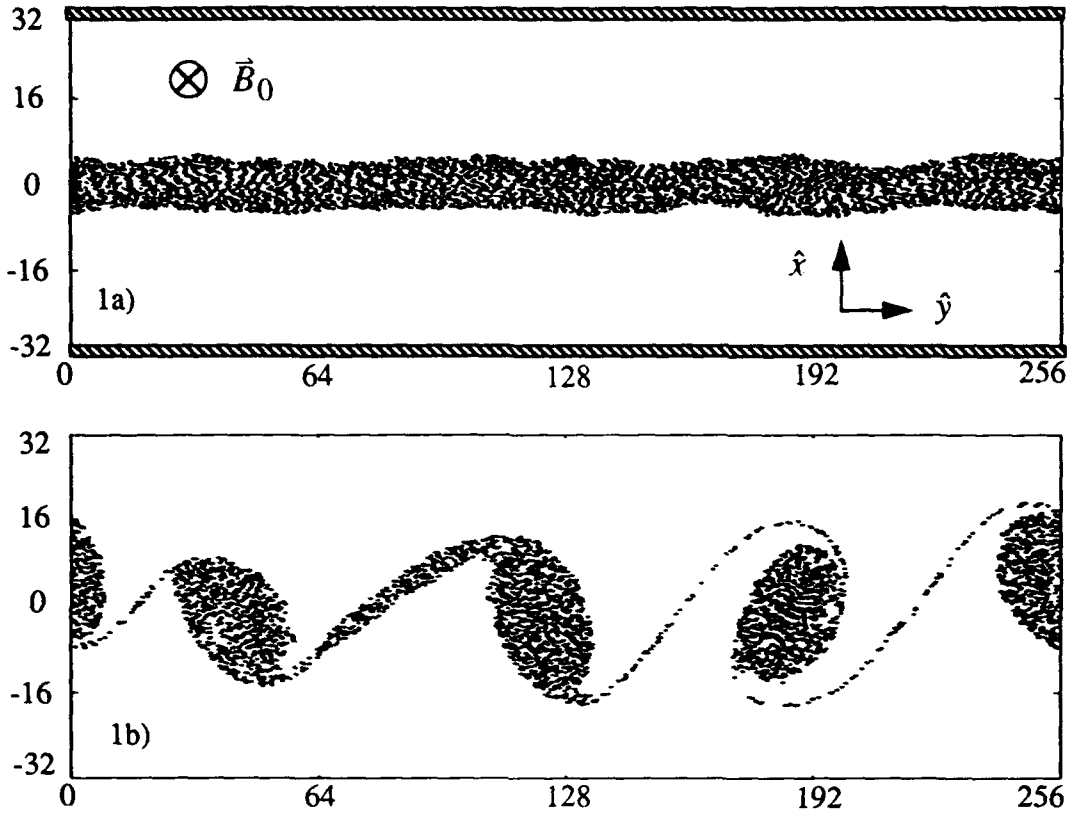

Fig 1: Nonneutral plasma slab simulation at 1a) time $t = 30$, and 1b) time $t = 70$. Spatial coordinates are scaled to Debye lengths, and $r_p/a = 0.15$.

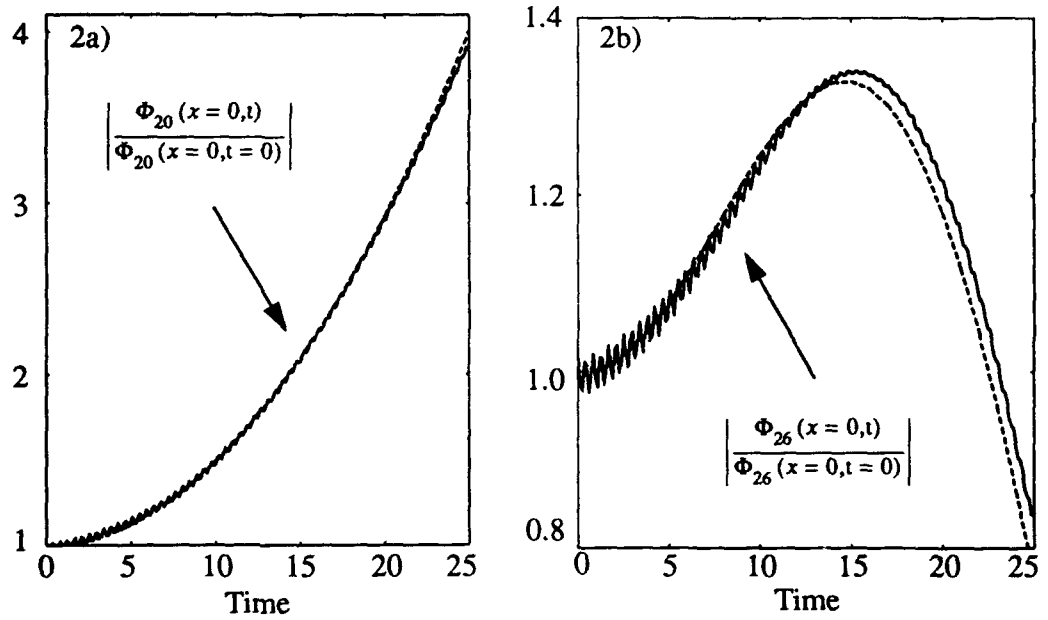

Fig 2: Initial-value theory (dashed line) and simulation data (solid line) along $x = 0$ for 2a) mode 20, and 2b) mode 26.

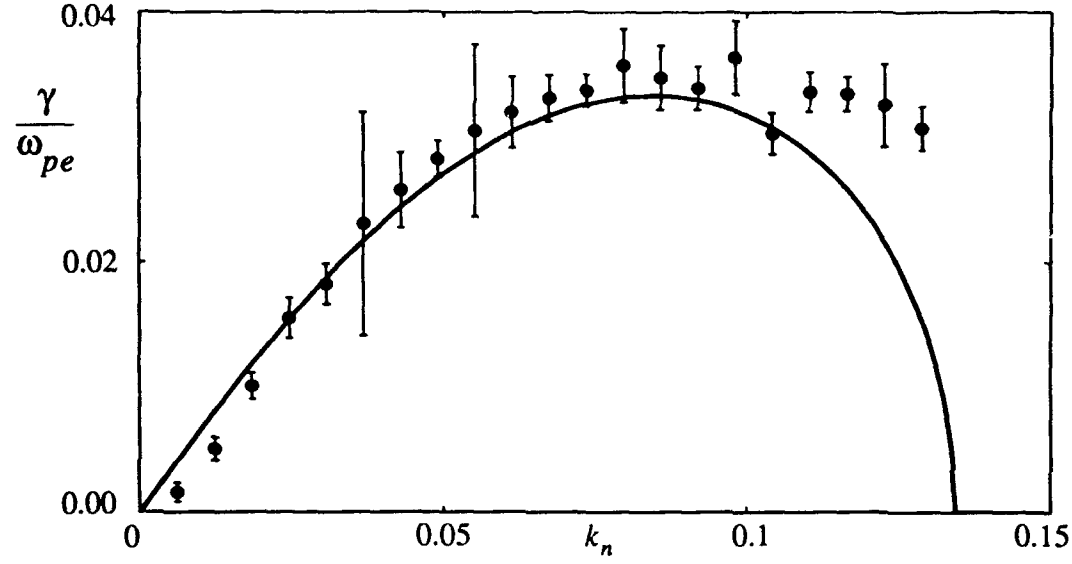

Fig. 3: Measured growth rates of the unstable modes of the nonneutral plasma slab in Figure 1.

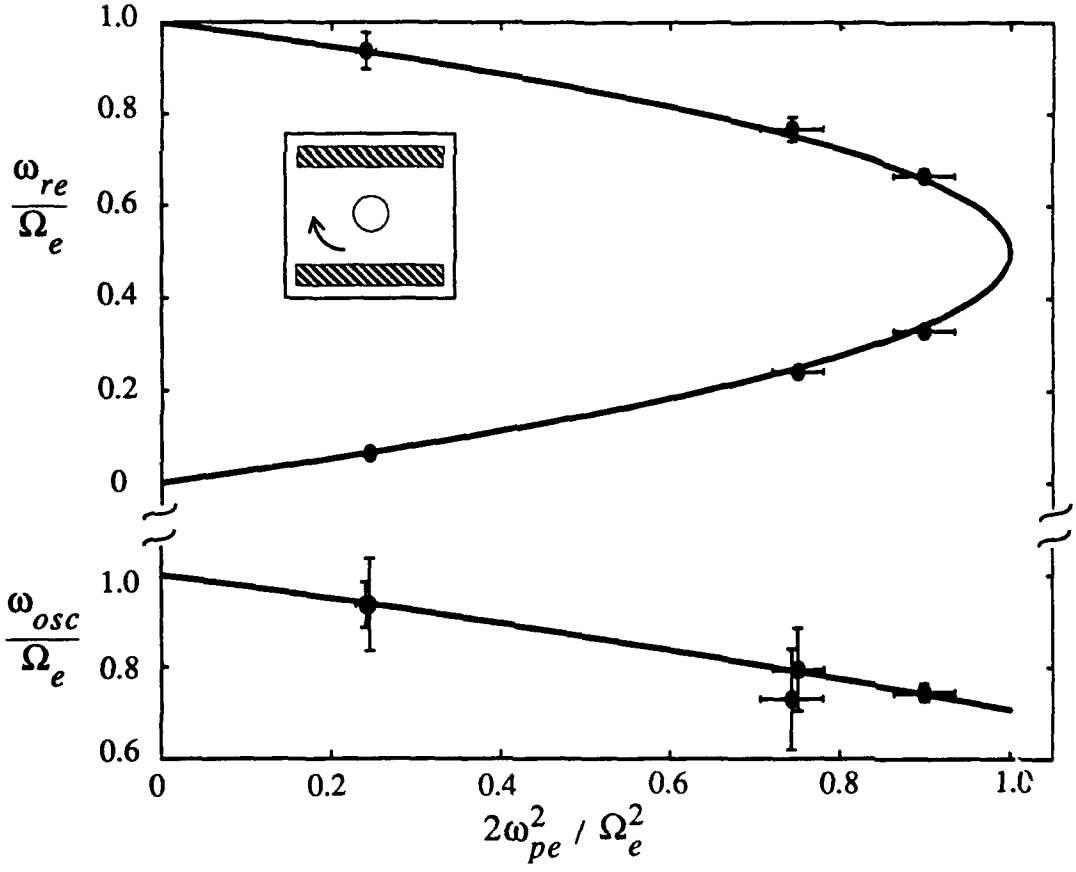

Fig 4: Measured equilibrium rotation frequencies and radial oscillation frequencies of the nonneutral rigid rotor.